Food Chemistry 119 (2010) 317–322

Contents lists available at ScienceDirect

Food Chemistry

journal homepage: www.elsevier.com/locate/foodchem

Impact of the crystallisation pathway of inulin on its mono-hydrate to hemi-hydrate thermal transition

Sébastien N. Ronkart [a,b,*], Claude Deroanne [a], Michel Paquot [b], Christian Fougnies [c], Christophe S. Blecker [a]

[a] Gembloux Agro-Bio Tech, University of Liège, Department of Food Technology, Passage des Déportés, 2, B-5030 Gembloux, Belgium
[b] Gembloux Agro-Bio Tech, University of Liège, Department of Industrial Biological Chemistry, Passage des Déportés, 2, B-5030 Gembloux, Belgium
[c] Cosucra Groupe Warcoing S.A., Rue de la Sucrerie, 1, B-7740 Warcoing, Belgium

ARTICLE INFO

Article history:
Received 15 March 2009
Received in revised form 25 May 2009
Accepted 17 June 2009

Keywords:
Inulin
Thermal properties
Hydrate
Crystallisation

ABSTRACT

In this paper, we present the thermal properties of two inulins obtained from different crystallisation pathways. One was obtained by fractional precipitation of a saturated inulin solution and the second was from the crystallisation of a solid amorphous inulin. The thermal analyses were conducted by temperature resolved wide angle X-ray scattering (TRWAXS), differential scanning calorimetry (DSC) and thermogravimetry (TG). Although at room temperature both inulins presented similar X-ray diffractogram patterns characteristic of the mono-hydrate polymorph, they differed considerably by their thermal properties. During heating, a difference in the mono-hydrate to the hemi-hydrate polymorph transition occurred. Thermogravimetric analysis suggested a difference in the water mobility inside the material which had an impact on the thermal properties and hydrate transition of the crystalline inulin.

1. Introduction

Polysaccharides are commonly used as ingredients or excipients in the food or pharmaceutical industries. They are usually produced in a powdered form (by techniques like spray-drying, freeze-drying, etc.) which has the advantage of facilitating manipulation, transport, storage and formulation. Depending on the processing or manufacturing, the powder can be partially or completely crystalline, which affects the technofunctional properties of the powder (Bhandari & Hartel, 2005). Polysaccharides are well known to present various crystalline polymorphs which have an impact on the solid-state properties of the powder, i.e. compressibility, dissolution, hygroscopicity, etc. (Bechtloff, Nordhoff, & Ulrich, 2001; Otsuka, Teraoka, & Matsud, 1991; Sun, 2006). The aim of this study is to investigate further the characterisation of thermal properties of polysaccharides presenting similar crystallinity contents but obtained by different crystallisation pathways. In particular, we want to emphasise the influence of the crystallisation pathway of polysaccharides on their thermal properties and polymorphic transitions. For this purpose, inulin, the most abundant non-structural carbohydrate in plants after starch was selected as a study model.

Inulin plays a major role in the food industry because it is considered to be a dietary fibre but is also used as a bulking agent and a fat or sugar substitute. As inulin is commercially available in the powdered form, it has also been proposed as an excipient for protein stabilisation in the pharmaceutical domain (de Jonge et al., 2007; Hinrichs, Prinsen, & Frijlink, 2001). It is composed of fructose unit chains (linked by (2 → 1)-β-D-fructosyl-fructose bonds) of various length terminated generally by a single glucose unit (linked by an α-D-glucopyranosyl bond) (French, 1993). The unit cell lattice of crystalline inulin is orthorhombic but depending on its hydration level, it can present two hydrates: a hemi-hydrate and a mono-hydrate (André, Mazeau et al., 1996; André, Putaux et al., 1996; Marchessault, Bleha, Deslandes, & Revol, 1980). According to the works of Marchessault et al. (1980), André, Putaux et al. (1996) and André, Mazeau et al. (1996), the main difference between the mono-hydrated and the hemi-hydrated polymorph does not correspond to any change in conformation of inulin, but rather to a variation in the number of water molecules in the unit cell, meaning a hydration state modification of the crystal without significant variations of the unit cell parameters.

In this study, two crystalline inulins of similar crystallinity and X-ray diffractogram pattern (characteristic of the mono-hydrate polymorph) were obtained from two different pathways: a fractional precipitation by cooling a saturated solution (Hébette et al., 1998; Ronkart et al., 2007) or from the solid-state by decreasing the glass transition temperature of the amorphous phase of the material below its storage temperature (Ronkart et al., 2006; Zimeri & Kokini, 2002). These two inulins were then analysed by

* Corresponding author. Address: Gembloux Agro-Bio Tech, University of Liège, Department of Food Technology, Passage des Déportés, 2, B-5030 Gembloux, Belgium. Tel.: +32 (81) 62 23 03; fax: +32 (81) 60 17 67.
E-mail address: ronkart.s@fsagx.ac.be (S.N. Ronkart).

0308-8146/$ - see front matter © 2009 Elsevier Ltd. All rights reserved.
doi:10.1016/j.foodchem.2009.06.035

wide angle X-ray scattering, differential scanning calorimetry, temperature resolved X-ray scattering and thermogravimetry.

2. Experimental section

The general strategy for the production and the characterisation of inulins is illustrated in Fig. 1.

2.1. Samples preparation

The starting inulin sample was a spray-dried product extracted from chicory roots kindly supplied by Cosucra Groupe Warcoing S.A. (Fibruline® XL, Warcoing, Belgium). The powder was dispersed in distilled water (to a solid concentration of 20%, w/w) at 40 or 95 °C, then spray-dried in a pilot plant scale Anhydro Lab S1 spray-drier (Anhydro, Denmark) from the Technological Center of Gembloux Agro-Bio Tech as described in Ronkart et al. (2007). The liquid feed flow and the air pressure nozzle flow were 2 l h^{-1} and 2 bars, respectively; while the inlet air temperature was set at 120 °C. The products are labelled 40/120 and 95/120, referring to the feed temperature (40 and 95 °C) and to the inlet air temperature of the spray-drier of 120 °C. Then, inulins were dried over P_2O_5 (one week) to obtain a dehydrated product, and then conditioned one week at 20 °C at 94% of relative humidity. The resulting products are named 40/120/94% and 95/120/94% in reference to the feed temperature, inlet air temperature and the relative humidity of the storage.

Finally, 40/120/94% and 95/120/94% were analysed by wide angle X-ray scattering (WAXS), temperature resolved wide angle X-ray scattering (TRWAXS), differential scanning calorimetry (DSC) and thermogravimetry (TG).

2.2. Wide angle X-ray scattering

The wide angle X-ray scattering apparatus was a PW3710 Philips Analytical X-ray B.V. with a Ni-filtered Cu Kα radiation (λ = 1.54178 Å), generated by an anode device operating at 40 kV and 30 mA in conjunction with a proportional detector. The patterns were recorded with a fixed time of 0.4 s per step of 0.02° in the $4° < 2\theta < 30°$ range, at 20 °C.

2.3. Differential scanning calorimetry

The thermal properties of powders were examined with a DSC 2920 TA Instruments (New Castle, DE) with a refrigerated cooling assessory and modulated capability. The cell was purged with 70 ml min^{-1} dry nitrogen, calibrated for baseline on an empty oven and for temperature using two standards (indium, T_{onset}: 156.6 °C; eicosane, T_{onset}: 36.8 °C). Specific heat capacity (C_p) was calibrated using a sapphire. The empty sample and reference pans were of equal mass to within ±0.10 mg. All measurements were made at least in triplicate using non-hermetic aluminium pans. The sample mass was weighed and was around 7 mg. The thermograms were obtained over a temperature range of 20–220 °C, with a heating rate of 1.5 °C min^{-1}, while the amplitude and the period of the modulation were 1.5 °C and 90 s, respectively.

2.4. Temperature resolved wide angle X-ray scattering

Temperature resolved wide angle X-ray scattering (TRWAXS) analysis were performed using an X'Pert Pro apparatus (PANalytical, Netherlands) equipped with an X'Celerator detector. The patterns were recorded in the $9.0° < 2\theta < 13.5°$ range (time scan = 60 s) from 25 to 200 °C. The heating rate was 1.5 °C min^{-1} and controlled with an Anton Paar TCU 100 (Graz, Austria).

2.5. Thermogravimetric analysis

Thermogravimetric analyses (TG) were performed using a TGA/DSC 1 (Mettler-Toledo). The analyses were conducted with a nitrogen flow of 35 and 100 ml min^{-1} for the protective and the purge gas, respectively. The apparatus was calibrated for temperature by using two standards (indium, T_{onset}: 156.6 °C; zinc, T_{onset}: 419.5 °C). The experiments were made at least in triplicate using

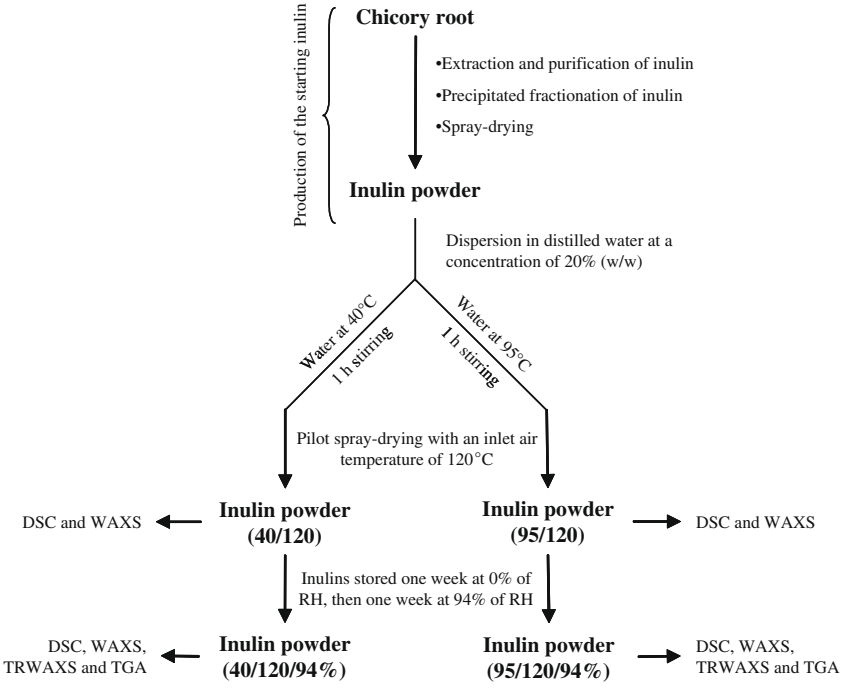

Fig. 1. General strategy for the production and the characterisation of inulins. MDSC: modulated differential scanning calorimetry; WAXS: wide angle X-ray scattering; TRWAXS: temperature resolved wide angle X-ray scattering; TGA: thermogravimetric analysis; RH: relative humidity.

aluminium pans without lids. The sample mass was precisely weighed and was around 15–20 mg. The thermograms were obtained over a temperature range comprised between 25 and 220 °C with a heating rate of 1.5 °C min^{-1}. To ascertain the molecular origin of the mass loses in the thermograms, a TGA/DSC 1 (Mettler Toledo, Switzerland) coupled to a mass spectrometer Thermostar (Balzers) was used.

3. Results and discussion

X-ray diffractograms of 40/120, 40/120/94%, 95/120 and 95/120/94% are presented in Fig. 2. In the $4° < 2\theta < 30°$ range, these inulins presented either a broad halo pattern or diffraction peaks, which is characteristic of an amorphous or a semi-crystalline state, respectively. As expected, 95/120 was initially completely amorphous, while 40/120 presented diffraction peaks which are characteristics of a semi-crystalline inulin. After one week of storage at 94% of relative humidity (RH), 40/120 and 95/120 were converted into 40/120/94% and 95/120/94% which both presented similar diffraction peak positions with roughly the same intensity (crystallinity index of ~92–97). Based on the position and the relative intensity of the inulin diffraction peaks published by André, Putaux et al. (1996), André, Mazeau et al. (1996), we can attribute the crystalline polymorph of 40/120, 40/120/94% and 95/120/94% to the mono-hydrated form. According to previous works on the solid-state of inulin (Ronkart, Paquot, Fougnies, Deroanne, & Blecker, 2009a; Schaller-Povolny, Smith, & Labuza, 2000; Zimeri & Kokini, 2002), amorphous inulin (but this is also applicable to other saccharides) picks up moisture from the surrounding air. In the present study, this moisture was from the high humidity storage of the inulin at 94% of RH. This water is absorbed by the amorphous part of inulin and acts as a plasticiser of the material, meaning that the glass transition temperature (T_g) of the amorphous product decreases (Roos & Karel, 1991). As reported in previous studies on inulin composed of an amorphous fraction (Ronkart, Deroanne, Paquot, & Blecker, 2009b; Ronkart et al., 2009a, 2009c), as soon as Tg dropped below the storage temperature, the powder crystallised, explaining why 95/120/94% as well as 40/120/94% were crystalline when 40/120 and 95/120 were stored at 94% of RH for one week.

DSC total heat flow curves of 40/120/94% and 95/120/94% are shown in Fig. 3. The full thermograms in the 20–220 °C range (Fig. 3a) allow the visualisation of water loss, crystal melting, and thermal degradation of inulins; whereas Fig. 3b focuses more particularly on their crystalline properties in the 120–190 °C range. Thermograms in Fig. 3b reveal an endothermic peak at T_2 = 157 °C for 40/120/94% and T_2 = 160 °C for 95/120/94% which is due to the melting of crystals formed during the one week storage at 94% of RH (Ronkart et al., 2009a). The thermogram of 40/120 (and 40/120/94%) was characterised by an extra dual endothermic peak (labelled peak 1 and 1′) at T_1 = 171–172 °C and T_1' = 178–179 °C, which corresponded to the melting of a double crystal population formed during the inulin manufacturing (crystallisation of the saturated inulin solution before its dehydration by spray-drying) (Hébette, 2002; Ronkart et al., 2007).

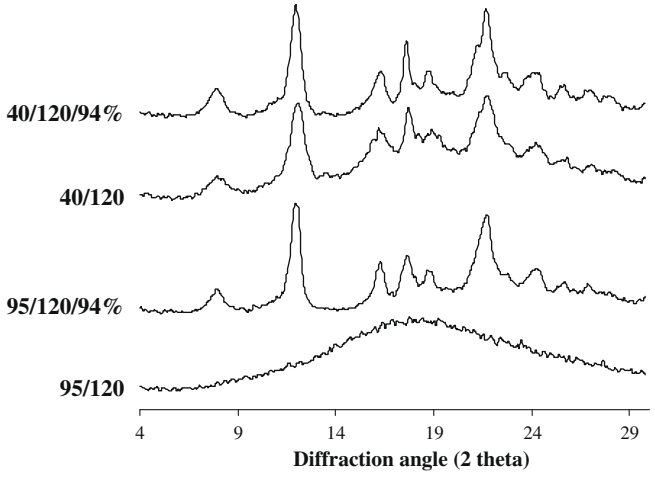

Fig. 2. Wide angle X-ray scattering diffractograms of: (a) 95/120, (b) 95/120/94%, (c) 40/120 and (d) 40/120/94%.

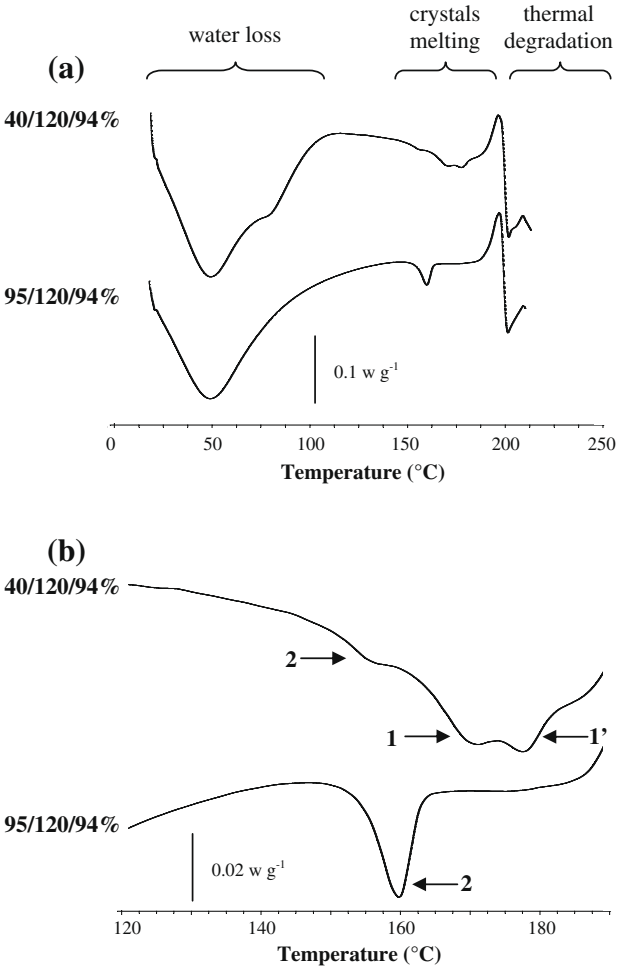

Fig. 3. Modulated differential scanning calorimetry thermograms of inulins in the: (a) 20–220 °C or (b) 120–190 °C range of: (1) 40/120/94% and (2) 95/120/94%.

Thus, although 40/120/94% and 95/120/94% presented the same diffraction peak features (Fig. 2), their DSC thermograms were different. In order to determine the impact of the temperature on the structural organisation of the molecules in the material, the X-ray diffractogram of 40/120/94% and 95/120/94% was analysed by TRWAXS with the same heating rate (1.5 °C min^{-1}) as used in the DSC (Fig. 4). Up to 145 °C, 95/120/94% showed diffraction peaks; while above this value, the diffraction peak intensity decreased. In comparison to the DSC results, the beginning and the end of the endothermic peak corresponded to the transition observed in the TRWAXS experiments (145 and 165 °C for onset and endset temperature, respectively). These results clearly indicated that this transition was due to a loss of the crystalline structure. Although similar results were observed for 40/120/94%, its total loss of crystallinity was shifted toward a higher temperature in comparison with 95/120/94% (Fig. 4), and corresponded to the melting of the

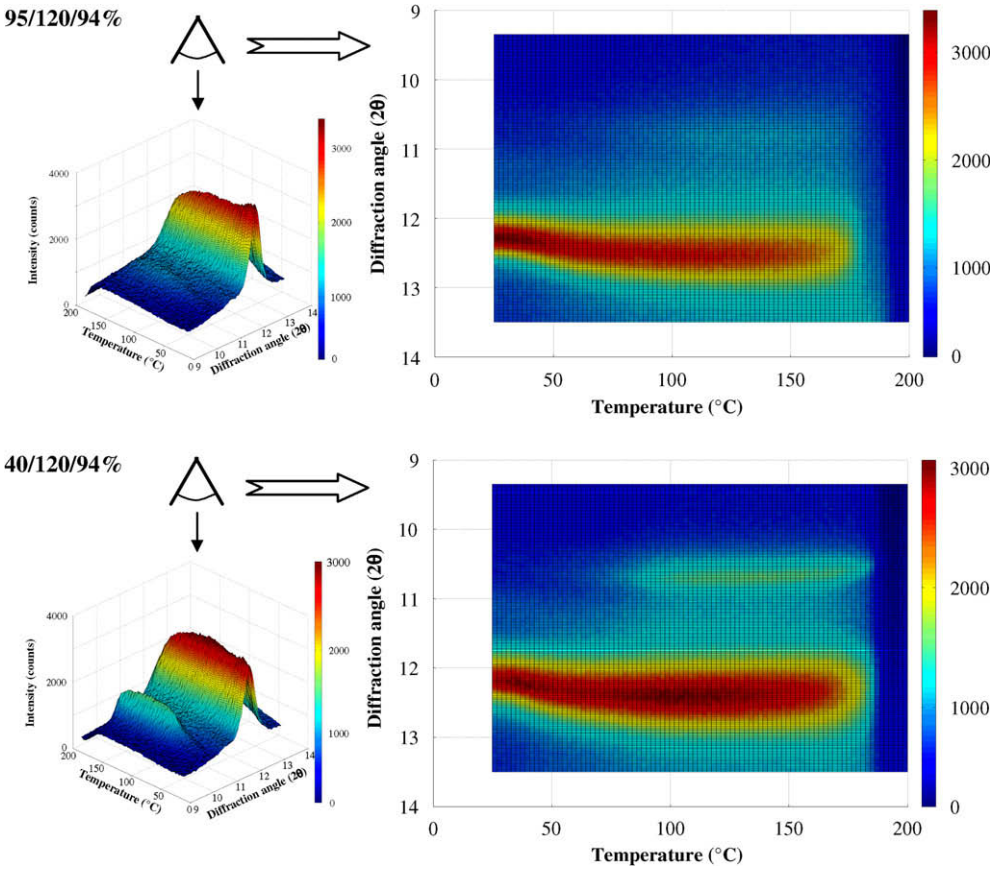

Fig. 4. Temperature resolved wide angle X-ray scattering patterns of: (a) 95/120/94% and (b) 40/120/94%.

dual endothermic peak centered at T_1 = 171–172 °C and T_1' = 178–179 °C (Fig. 3). During heating, a diffraction peak centered at $2\theta = 10.6°$ appeared for 40/120/94% (Fig. 4b) and characterised a transition from the mono-hydrate to the hemi-hydrate polymorph, meaning a hydration state change of the crystal without significant modifications of the unit cell parameters. Although 95/120/94% was also initially characterised by the mono-hydrate polymorph (before heating), no clear pseudo-polymorphic transition was observed during TRWAXS experiments (Fig. 4a). Such a difference between 40/120/94% and 95/120/94% was probably due to a difference in the powder stability due to the high humidity storage. Indeed, although they presented the same diffraction peak patterns, most of the crystals of 40/120/94% were formed during the precipitation of an oversaturated solution of inulin (fractional precipitation of inulin) before spray-drying, while those of 95/120/94% were from the crystallisation of amorphous inulin in the solid-state. It resulted in a caking of the powders for both 40/120/94% and 95/120/94%, but the significance of this phenomenon depended on the amorphous / crystallinity content of inulin before the 94% RH storage (Ronkart et al., 2009c). Indeed, a continuous mass was observed for 95/120/94% (the particles composing the powder were fused together), while 40/120/94% was slightly agglomerated and the entire inulin powder was easily recoverable. Such a difference in the extent of caking could have an impact on the water mobility/migration inside the material during thermal analysis and thus an impact on the hydration state change of the crystals. For this reason, water loss profiles of 40/120/94% and 95/120/94% were investigated by thermogravimetry (TG). The choice of this technique was motivated by the work of Men and Rieger (2004) who correlated TRWAXS and TG results to understand crystalline transition in polyamide (PA6/66) copolymer and also the water mobility of the polymer during heating. These authors pointed out polymorphic transitions of the polymer during heating, but also emphasised the importance of the hydration state on the crystalline structure changes.

TG thermograms of 40/120/94% and 95/120/94% are presented in Fig. 5 and show two or three major weight loses. The first started from the beginning of the running experiment at 25 °C to 90–95 °C for 40/120/94%. The associated mass loss was 17.18 ± 0.88% and is probably due to bound water. According to Hu, Kaplan, and Cebe (2007), this water is easily eliminated by conditioning the sample in a dehydrating atmosphere such as in a desiccator for example. However, 95/120/94% presented a continuous weight mass loss of 17.23 ± 0.31% up to 180 °C (note that this temperature corresponded to the beginning of the thermal degradation of inulin). The TG thermograms could explain the hydration state change of 40/120/94% observed by TRWAXS (lower left frame inlay of Fig. 5). Indeed, the end of the first water mass loss of 40/120/94% occurred at around 90–95 °C which corresponded to the beginning of the transition from the mono- to the hemi-hydrate form (Fig. 4b). On the other hand, 95/120/94% still presented a water loss up to the inulin degradation (at around 180 °C). No hydration state transition from the mono to the hemi-hydrate was observed for 95/120/94% during TRWAXS analysis (Fig. 4a) probably due to the permanent trace of water.

A second mass loss of 0.31 ± 0.02% occurred in the TG thermogram in the 160–180 °C range for 40/120 and is presented in the upper right frame inlay of Fig. 5. Although such a transition could be attributed to a degradation event, as observed elsewhere on an encapsulated drug in a polymer (Silva-Júnior et al., 2008), it was due in our case to water evaporation. The origin of this volatile compound was confirmed by thermogravimetry coupled to a mass

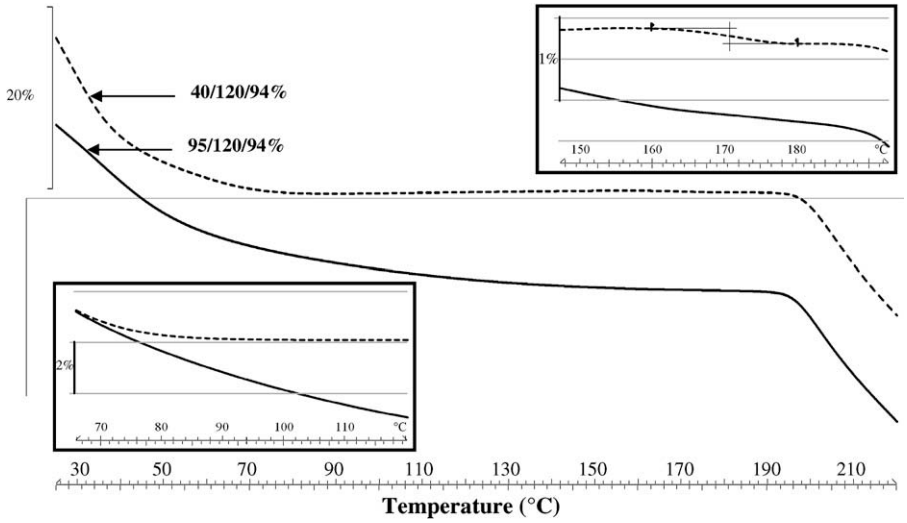

Fig. 5. Thermogravimetric curves of the weight loss of 40/120/94% (dashed lines) and 95/120/94% (solid lines) in the 25–220 °C. Lower left frame inlay illustrates the end of the first water loss of 40/120/94% at around 90–95 °C, while 95/120/94% shows a continuous water mass loss up to 180 °C. Upper right frame inlay illustrates the water loss step of 40/120/94% in the 160–180 °C range.

spectrometer (data not shown). Indeed, the mass spectra recorded at a mass to charge ratio m/z of 17 and 18 (characteristic of water molecular mass) were recorded and correlated to the mass weight loss determined by TG in Fig. 5. This water loss is associated to hydrate water from the hemi-hydrate polymorph crystals during their melting. This fact was supported by the DSC curve of 40/120/94% (Fig. 3b) which showed the melting of the crystals in the same temperature range of 140–160 °C.

Finally, a third mass loss step starting at 180 °C for both 40/120/94% and 95/120/94% was ascertained by mass spectrometry as inulin thermal degradation. This thermal degradation of inulin has been described by Bohm, Kaiser, Trebstein, and Henle (2005) as the breakdown of the long fructose chains and the formation of di-D-fructose dianhydrides. In such conditions, a browning of inulin was observed for both 40/120/94% and 95/120/94%.

4. Conclusions

In this study, we reported the impact of the crystallisation pathway of polysaccharides on their thermal and polymorphic properties. Two inulins which presented the same molecular organisation and roughly crystallinity content (crystallinity index: ~92–97) were produced. One was obtained by the precipitation of an oversaturated solution while the second was a molecular arrangement of the solid amorphous state. It led to a change on the water mobility inside the material which modified the polymorphism of inulin crystals, as well as their melting behaviour. These results are interesting to the industry because it is well known that a difference in the polymorphism induces technofunctionality changes of the powder (such as hygroscopicity, solubility, etc.) during processing or formulation of the powder.

Acknowledgments

The authors are grateful to the 'Department of Structural Biological Chemistry' of 'The University Faculties of Notre Dame de la Paix' (Namur, Belgium) for the X-ray facilities; David Ooms from the 'Unité de Mécanique et Construction' of the 'Gembloux Agricultural University' for his help with the graphical design; Philippe Larbanois (Mettler Toledo, Belgium) and Kai Hassdenteufel (Mettler Toledo, Switzerland) for their help with the TG-MS. C.S. B. acknowledges the Fonds de la recherche Scientifique – FNRS for the financial support of the TGA.

Appendix

40/120	inulin produced by pilot spray-drying with a feed temperature of 40 °C and an inlet air temperature of 120 °C
40/120/94%	inulin produced by pilot spray-drying with a feed temperature of 40 °C and an inlet air temperature of 120 °C, then stored one week at a relative humidity of 94%
95/120	inulin produced by pilot spray-drying with a feed temperature of 95 °C and an inlet air temperature of 120 °C
95/120/94%	inulin produced by pilot spray-drying with a feed temperature of 95 °C and an inlet air temperature of 120 °C, then stored one week at a relative humidity of 94%
θ	theta angle
°	degree
Cp	specific heat capacity
DSC	differential scanning calorimetry
m/*z*	mass to charge ratio
RH	relative humidity
T_g	glass transition temperature
T_{onset}	onset temperature
TG	thermogravimetry
TRWAXS	temperature resolved wide angle X-ray diffraction
WAXS	wide angle X-ray diffraction

References

André, I., Mazeau, K., Tvaroska, I., Putaux, J. L., Winter, W. T., Taravel, F. R., et al. (1996b). Molecular and crystal structures of inulin from electron diffraction data. *Macromolecules, 29*, 4626–4635.

André, I., Putaux, J. L., Chanzy, H., Taravel, F. R., Timmermans, J. W., & de Wit, D. (1996a). Single crystals of inulin. *International Journal of Biological Macromolecules, 18*, 195–204.

Bechtloff, B., Nordhoff, S., & Ulrich, J. (2001). Pseudopolymorphs in industrial use. *Crystal Research and Technology, 36*, 1315–1328.

Bhandari, B. R., & Hartel, R. W. (2005). Phase transitions during food powder production and powder stability. In C. Onwulata (Ed.). *Encapsulated and powdered foods* (pp. 261–291). New York: Taylor and Francis.

Bohm, A., Kaiser, I., Trebstein, A., & Henle, T. (2005). Heat-induced degradation of inulin. *European Food Research and Technology, 220*, 466–471.

de Jonge, J., Amorij, J.-P., Hinrichs, W. L. J., Wilschut, J., Huckriede, A., & Frijlink, H. W. (2007). Inulin sugar glasses preserve the structural integrity and biological activity of influenza virosomes during freeze-drying and storage. *European Journal of Pharmaceutical Sciences, 32*, 33–44.

French, A. D. (1993). Recent advances in the structural chemistry of inulin. In A. Fuchs (Ed.), *Inulin and inulin-containing crops* (pp. 121–127). Amsterdam: Elsevier Sciences Publishers B.V.

Hébette, C. (2002). *Crystallisation, melting and gel formation of concentrated inulin-water systems*. PhD Thesis. K.U. Leuven: Belgium.

Hébette, C. L. M., Delcour, J. A., Koch, M. H. J., Booten, K., Kleppinger, R., Mischenko, N., et al. (1998). Complex melting of semi-crystalline chicory (*Cichorium intybus* L.) root inulin. *Carbohydrate Research, 310*(6), 5–75.

Hinrichs, W. L. J., Prinsen, M. G., & Frijlink, H. W. (2001). Inulin glasses for the stabilization of therapeutic proteins. *International Journal of Pharmaceutics, 215*, 163–174.

Hu, X., Kaplan, D., & Cebe, P. (2007). Effect of water on the thermal properties of silk fibroin. *Thermochimica Acta, 461*, 137–144.

Marchessault, R. H., Bleha, T., Deslandes, Y., & Revol, J. F. (1980). Conformation and crystalline structure of (21)-D-fructofuranan (inulin). *Canadian Journal of Chemistry, 58*, 2415–2422.

Men, Y., & Rieger, J. (2004). Temperature dependent wide angle X-ray diffraction studies on the crystalline transition in water saturated and dry polyamide 6/66 copolymer. *European Polymer Journal, 40*, 2629–2635.

Otsuka, M., Teraoka, R., & Matsud, Y. (1991). Physicochemical properties of nitrofurantoin anhydrate and monohydrate and their dissolution. *Chemical and Pharmaceutical Bulletin, 39*, 2667–2670.

Ronkart, S., Blecker, C., Fougnies, C., Van Herck, J.-C., Wouters, J., & Paquot, M. (2006). Determination of physical changes of inulin related to sorption isotherms: An X-ray diffraction, modulated differential scanning calorimetry and environmental scanning electron microscopy study. *Carbohydrate Polymers, 63*, 210–217.

Ronkart, S. N., Deroanne, C., Paquot, M., & Blecker, C. S. (2009b). Phénomène de la transition vitreuse appliquée aux glucides alimentaires amorphes à l'état de poudre. *Biotechnologie Agronomie Société et Environnement*.

Ronkart, S. N., Deroanne, C., Paquot, M., Fougnies, C., Lambrechts, J.-C., & Blecker, C. (2007). Characterization of the physical state of spray-dried inulin. *Food Biophysics, 2*, 83–92.

Ronkart, S. N., Paquot, M., Blecker, C. S., Fougnies, C., Doran, L., Lambrechts, J.-C., et al. (2009c). Impact of the crystallinity on the physical properties of inulin during water sorption. *Food Biophysics, 4*, 49–58.

Ronkart, S. N., Paquot, M., Fougnies, C., Deroanne, C., & Blecker, C. S. (2009a). Effect of water uptake on amorphous inulin properties. *Food Hydrocolloids, 23*, 922–927.

Roos, Y., & Karel, M. (1991). Water and molecular weight effects on glass transitions in amorphous carbohydrates and carbohydrate solutions. *Journal of Food Science, 56*, 1676–1681.

Schaller-Povolny, L. A., Smith, D. E., & Labuza, T. P. (2000). Effect of water content and molecular weight on the moisture isotherms and glass transition properties of inulin. *International Journal of Food Properties, 3*, 173–192.

Silva-Júnior, D. A. A., Scarpa, M. V., Pestana, K. C., Mercuri, L. P., de Matos, J. R., & de Olivera, A. G. (2008). Thermal analysis of biodegradable microparticles containing ciprofloxacin hydrochloride obtained by spray drying technique. *Thermochimica Acta, 467*, 91–98.

Sun, C. (2006). Solid-state properties and crystallization behaviour of PHA-739521 polymorphs. *International Journal of Pharmaceutics, 319*, 114–120.

Zimeri, J. E., & Kokini, J. L. (2002). The effect of moisture content on the crystallinity and glass transition temperature of inulin. *Carbohydrate Polymers, 48*, 299–304.